

# SIMULATION OF DETERRENT DIFFUSION IN DOUBLE BASE PROPELLANT UNDER DIFFERENT TEMPERATURE PROFILES

Bertrand Roduit<sup>1</sup>, Rainer Brandsch<sup>2</sup>, Patrick Folly<sup>3</sup>, Alexandre Sarbach<sup>3</sup>, Beat Berger<sup>3</sup>, Beat Vogelsanger<sup>4</sup>, Bruno Ossola<sup>4</sup>, Laurence Jeunieau<sup>5</sup>, Pierre Guillaume<sup>6</sup>,

<sup>1</sup>AKTS AG, <http://www.akts.com>, TECHNOArk 1, 3960 Siders, Switzerland, [b.rodut@akts.com](mailto:b.rodut@akts.com)

<sup>2</sup>MDCTec Systems GmbH, Gutenbergstrasse 5, 82205 Gilching, Germany

<sup>3</sup>armasuisse, Science and Technology Centre, 3602 Thun, Switzerland

<sup>4</sup>Nitrochemie Wimmis AG, 3752 Wimmis, Switzerland

<sup>5</sup>Royal Military Academy, Avenue de la Renaissance 30, 1000 Bruxelles, Belgium

<sup>6</sup>PB Clermont s.a., Rue de Clermont 176, 4480 Engis, Belgium

## Abstract

Propellants can burn so rapidly that the initial rise of pressure in weapons may be faster than desired. To avoid this unwanted effect, burning rate of the propellants is moderated by applying a surface coating. Coating agents are usually deterrents (moderants), substances that gelatinize or plasticise the nitrocellulose matrix of the propellants decreasing its initial burning rate, therefore, in turn, the rate of gaseous phase formation. The knowledge of the diffusion rate of deterrents helps therefore in developing propellants with superior ballistic performance. Another parameter, namely the rate of the migration of deterrent into the propellant matrix during ageing / storing is also important as it influences the ballistic shelf-life i.e. the period of time during which the ballistic requirements are fulfilled. As migration measurements are often difficult, expensive and time-consuming the development of the simulation tools of above processes seems to be of a great importance. The present paper describes the simulation method for deterrent and blasting oil diffusion in double base propellant applying the temperature dependence of the diffusion coefficients  $D$  determined in isothermal experiments and taking into account the influence of the swelling effect of the propellant matrix. The simulations were done using the AKTS-SML software [1], which allowed considering the migration of both, deterrent and nitroglycerine through the swollen matrix of the propellant. Furthermore, after determination of the temperature dependence of the diffusion coefficient  $D$ , it was possible to predict the deterrent migration under any, arbitrarily chosen temperature profile such as oscillatory temperature mode, real atmospheric temperature profiles or under temperature mode corresponding to atmospheric changes according to STANAG 2895 [2].

## 1. Introduction

The interior ballistic performance of propellants can be significantly improved by the application of blasting oils and/or deterrents. However, the diffusion of these coating agents from the surface into the propellant grains during long-time storage may significantly reduce the shelf life of the propellant. The producers of propellants are responsible to ensure that their products meet the requirements in terms of deterrent migration over shelf life by taking into account the ballistic performance.

The deterrent diffusion was investigated in our previous studies [3-5] for various propellants containing approximately 5% - 15% nitroglycerine (NG). The concentration of deterrent, dibutylphthalate (DBP) or polymeric plasticizer, was 2% – 5%. The diffusion process was investigated by FTIR Microspectroscopy [6] in samples aged in isothermal conditions in the range of 50-80°C. For the samples containing DBP, the aging time, depending on the temperature, varied between 1-200 days, at the highest temperature of 80°C the aging time was between 1-11 days. It was experimentally found that the change of the deterrent concentration from the surface inwards was consistent with Fick's diffusion law, therefore the equation for one-dimensional diffusion in an anisotropic medium could be analytically solved. The average values of the diffusion coefficients obtained under isothermal conditions varied between about  $4.10^{-18}$  to  $7.2.10^{-16}$  m<sup>2</sup>/s at 50 and 80°C, respectively.

The present work was undertaken to further develop the potential of an existing simulation programme (AKTS-SML) in order to predict of the migration of deterrent and blasting oils inside propellant structures under non-steady experimental conditions (e.g. temperature fluctuations during the aging time, swelling effects). This study reports the possibilities and limitations of such simulations and presents their comparison with the experimental diffusion data.

## **2. Correlation between diffusion effects and ballistic stability**

Surface modification of propellant usually consists of an impregnation by a deterrent, which is only present along the surface up to a certain depth and with a certain gradient. This gradient allows tailoring of the burning rate during the combustion process. The service life of propellants is determined by two components: the chemical shelf life and the functional or ballistic shelf life.

- *The chemical shelf life* covers the period of time during which the propellant can be safely stored without causing hazards to its environment. This time is dependent on the extent of chemical ageing reactions, such as decomposition of nitric esters and reactions of the decomposition products with the stabilizer. The chemical stability can be assessed by heat flow calorimetry measurements and by monitoring stabilizer depletion. Results of such studies were reported in [7-10].

- *The functional or ballistic shelf life* is the period of time during which the propellant or ammunition can be used safely or during which the ballistic requirements remain fulfilled. The main propulsion-related factors which limit the functional life are incompatibility and migration processes and, to some extent, the partial decomposition of nitrocellulose [3-5].

The ballistic stability of the bullet depends principally on the degree of the deterrent migration rather than on the chemical stability of the propellant. The correlation between the maximal pressure in the cartridge and the concentration of deterrent at the surface of the grains was presented [3-5]. Therefore, the understanding of migration processes of deterrent and blasting oil in the nitrocellulose matrix is of great importance.

### 3. Diffusion models for monolayer bulk materials without swelling effect

Migration in bulk materials under isothermal conditions can be simulated by a simple diffusion model limited to monolayer cases where an analytical solution of the equations of diffusion, Fick's equations, can be derived [11].

Although the analytical solutions of the differential equations which describe the diffusion processes are known and can be found in many reference books, it is often difficult to extract the diffusion coefficient  $D$  from the experimental data. To obtain  $D$ , it is necessary to measure a *diffusion curve* or *concentration profile*, either in function of the diffusion time or in function of the diffusion path. Usually, the amount of substance which has migrated into the bulk material  $M(t)$  is measured in function of the time, or the concentration of this substance is measured along the diffusion path at a given time  $C(x,t)$ . Another parameter which has to be considered is the geometry of the system in which the diffusion process occurs. The solutions of the differential equations describing the diffusion in the system with geometry of plane sheet, cylinder and sphere are following [11-12]:

Diffusion from an infinite liquid into:

- a finite *plane sheet* with two sides contact:

$$\frac{M_t}{M_\infty} = 1 - \left( \frac{8}{\pi^2} \cdot \sum_{n=0}^{\infty} \frac{1}{(2n+1)^2} \cdot e^{-\frac{(2n+1)^2 \cdot \pi^2}{L^2} \cdot D \cdot t} \right) \quad (1)$$

or

$$C_{x,t} = C_1 - (C_1 - C_i) \cdot \left[ \frac{4}{\pi} \cdot \sum_{n=0}^{\infty} \frac{1}{(2n+1)} \cdot \sin\left(\frac{(2n+1) \cdot \pi \cdot x}{L}\right) \cdot e^{-\frac{(2n+1)^2 \cdot \pi^2}{L^2} \cdot D \cdot t} \right] \quad (2)$$

- a finite *plane sheet* with one side contact:

$$\frac{M_t}{M_\infty} = 1 - \left( \frac{8}{\pi^2} \cdot \sum_{n=0}^{\infty} \frac{1}{(2n+1)^2} \cdot e^{-\frac{(2n+1)^2 \cdot \pi^2}{4L^2} \cdot D \cdot t} \right) \quad (3)$$

or

$$C_{x,t} = C_1 - (C_1 - C_i) \cdot \left[ \frac{4}{\pi} \cdot \sum_{n=0}^{\infty} \frac{1}{(2n+1)} \cdot \sin\left(\frac{(2n+1) \cdot \pi \cdot x}{2L}\right) \cdot e^{-\frac{(2n+1)^2 \cdot \pi^2}{4L^2} \cdot D \cdot t} \right] \quad (4)$$

- a *cylinder* of finite length with radial and longitudinal diffusion:

$$\frac{M_t}{M_\infty} = 1 - \left\{ \left[ \frac{8}{\pi^2} \cdot \sum_{n=0}^{\infty} \frac{1}{(2n+1)^2} \cdot e^{-\frac{(2n+1)^2 \cdot \pi^2}{4L^2} \cdot D \cdot t} \right] \cdot \left[ 4 \cdot \sum_{n=1}^{\infty} \frac{1}{(\alpha_n R)^2} \cdot e^{-\frac{(\alpha_n R)^2}{R^2} \cdot D \cdot t} \right] \right\} \quad (5)$$

- into a *sphere*:

$$\frac{M_t}{M_\infty} = 1 - \frac{6}{\pi^2} \cdot \sum_{n=1}^{\infty} \frac{1}{n^2} \cdot e^{-\frac{D \cdot n^2 \cdot \pi^2 \cdot t}{R^2}} \quad (6)$$

or

$$C_{r,t} = C_1 - (C_1 - C_i) \left[ 1 + \frac{2 \cdot R}{\pi \cdot r} \sum_{n=1}^{\infty} \frac{(-1)^n}{n} \cdot \sin\left(\frac{n \cdot \pi \cdot r}{R}\right) \cdot e^{-\frac{n^2 \cdot \pi^2}{R^2} \cdot D \cdot t} \right] \quad (7)$$

where  $M(t)$  denotes the amount of diffusing substance which has diffused into the material (plane, cylinder or sphere) at diffusion time  $t$ ;  $M_{\infty}$ , the corresponding quantity after an infinite time and  $D$  the diffusion coefficient of the substance in the material.  $C(x,t)$  is the concentration of the diffusing substance at distance  $x$  from the surface at time  $t$ ; for a sphere  $C(r,t)$  is the concentration of the diffusing substance at radial distance  $r$  from the centre at time  $t$ ;  $C_1$  is the concentration at the surface and  $C_i$ , its initial concentration in the material.  $L$  is the thickness of the plane sheet or half the height of the cylinder and  $R$  is the radius of the sphere or the cylinder. The term  $\alpha_n R$  represents the roots of the Bessel function of first kind of order zero. The zeros were calculated in the program with an approximation which can be found in [13]. To estimate the best diffusion coefficient fitting the experimental data points, the AKTS-SML software uses a non linear regression algorithm of Levenberg-Marquardt. This method varies progressively  $D$  in order to minimize the sum of the squared difference between the measured and the calculated values [14]. Limitations of above equation during simulations are the following:

- the diffusion process has to occur in monolayer structures by following the Fick' Laws
- the diffusion coefficient must be constant during the course of the experiment
- no other phenomena contribute to the transfer of matter as e.g. evaporation on the surface or chemical reaction between matrix and diffused molecules or between different migrating compounds.

## 4. Diffusion models for single and/or multilayer bulk structures with swelling effect

### 4.1 The mathematical model

To simulate the migration process of deterrents and blasting oils in a propellant matrix it is necessary to take into account possible effect between matrix and diffused molecules or between different migrating compounds which will change the diffusion coefficient and, in turn, the concentration profiles of both deterrent and blasting oils. This can be done by solving the general form of Fick's Partial Differential Equations (PDE) applying numerical approximations:

$$\frac{\partial c}{\partial t} = \frac{\partial}{\partial r} \left( D(c, c_i, T) \frac{\partial c}{\partial r} \right) + \frac{g}{r} D(c, c_i, T) \frac{\partial c}{\partial r} \quad (8)$$

where  $g$  is a geometry factor dependent on the geometry of the propellant grain:  $g=0$  for an infinite plate,  $g=1$  for an infinite cylinder and  $g=2$  for a sphere.

$c$  = concentration of the migrant e.g. blasting oil at penetration depth  $r$  and time  $t$

$c_i$  = concentration of another migrant e.g. deterrent at penetration depth  $r$  and time  $t$

$T$  = temperature profile as a function of time  $t$

$D$  = diffusion coefficient that might depend on the concentration of a migrant  $c$  (e.g. blasting oil), or another migrant  $c_i$  (e.g. deterrent) and on the temperature  $T$ .

## 4.2 Diffusion of deterrents and blasting oils in double base or EI-propellants

The composition of propellants is rather complex which makes the study of the relationship between their properties and composition very difficult. Such phenomena like continuous change of the concentration of deterrent and blasting oil along the grain diameter and/or presence of the stabilizers etc. complicate the drawing of conclusions from the experimental observations. In order to validate the correctness and accuracy of the performed simulations the calculated data were compared with the results of experimental investigations reported in our previous studies [3-5]. Generally, the deterrent and blasting oils concentration profiles were measured by FTIR spectroscopy combined with infrared microscopy.

### 4.2.2 Diffusion processes during surface coating

A two-step surface coating process is mainly used in the production of double base propellants of EI-type [3-4]. The impregnation of single base propellant grains with blasting oil forms an outer layer with a thickness up to several hundred micrometers and almost uniform blasting oil concentration of 10 - 20% [3-4]. An example of such a concentration profile of blasting oil (here nitroglycerine) is presented in figure 1A. Following the impregnation process, the propellant grains are impregnated in a second step by the deterrent causing a nitroglycerine front movement towards the centre of the grains by some tens of micrometers. Deterrent and nitroglycerine concentration profiles are shown in figure 1 B (experimental data source: Nitrochemie Wimmis, Switzerland, [3-4]).

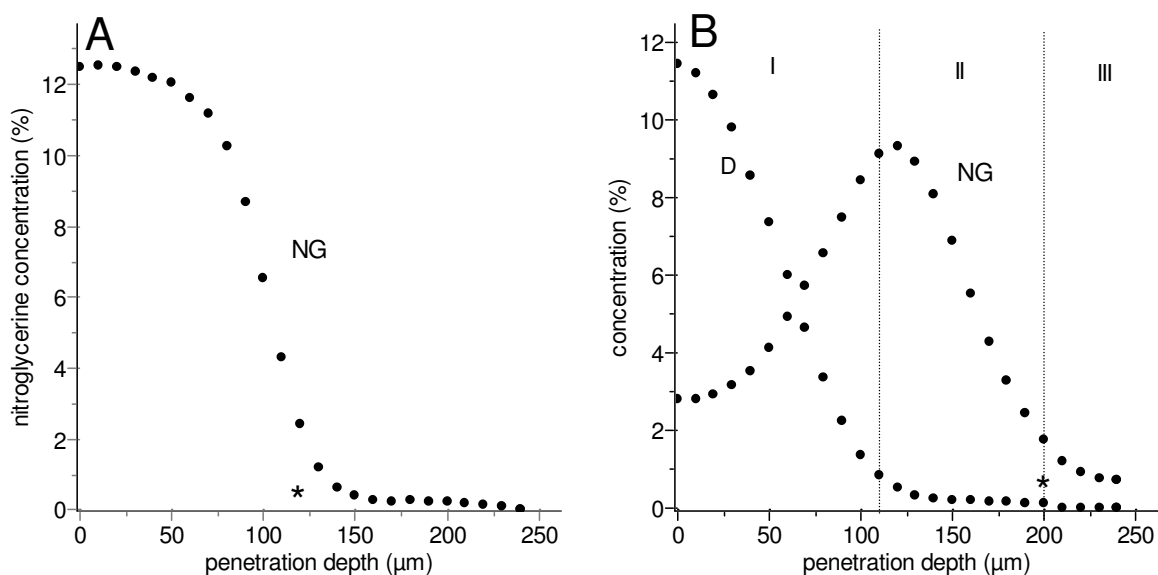


**Fig. 1** A) Nitroglycerine concentration profile after the first step of the EI surface coating process. The concentration of the nitroglycerine on the grain surface amounts to ca. 12.5%. B) Deterrent and nitroglycerine concentration profiles of an unaged EI-propellant after the second coating step. During the deterring process, the nitroglycerine front was shifted towards the centre of the grain by about 70 μm. The concentrations profiles measured by FTIR microscopy are displayed as dots, the positions of the nitroglycerine front as visible in optical microscopy are marked by asterisks in both figures.

In a rough approximation, the double base EI-propellant grains may be divided into three zones. In the outer layer (zone I), the nitrocellulose (NC) matrix contains nitroglycerine (NG) and polymeric deterrent, the latter in higher concentration (about 11% on the grain surface). Further inwards, a ring of

propellant containing NC and NG is present (zone II). Here, the nitroglycerine concentration is higher than in the outer zone. The inner core of the grains (zone III) consists of the original single base (NC) propellant matrix. A similar three-layer system was found by Levy [15] in some types of ball propellants using optical microscopy.

### 4.2.3 Diffusion processes during thermal aging

#### 4.2.3.1 Concentration distributions of deterrents and blasting oils

The diffusion rate of both monomeric and polymeric deterrents in single base propellants was found to be extremely small as reported in [3,4] where  $D_D$  value of  $1 \cdot 10^{-17} \text{ m}^2/\text{s}$  at  $71^\circ\text{C}$  was obtained. However, the diffusion rate of polymeric deterrents in nitrocellulose-blasting oil matrix (EI-propellants) turned out to be significantly higher than in single base propellants, with  $D$ -values laying in the range  $0.1 - 2 \cdot 10^{-15}$  at  $71^\circ\text{C}$  [3,4]. This phenomenon results from the fact that the nitrocellulose matrix is swollen due to the presence of NG in EI- or double base propellants. It is well known that the diffusion rate of any deterrent strongly depends on the degree of swelling by nitroglycerine: it is very low if NC matrix is not swollen (single base), intermediate-fast for an intermediate NG concentration (5-15%), and very fast for high concentration of NG (40%). Therefore, following simplified expression concerning the overall diffusion coefficient of deterrent can be proposed:

$$D_{D,total} = D_{D,1} + D_{D,2} \quad (9)$$

with

$$D_{D,1} = D_{D, \text{single base}} \quad (10)$$

$$D_{D,2} = D_{D, \text{double base}} \cdot \theta_{NG} \quad (11)$$

where  $\theta_{NG}$  is a factor characterizing the swelling of nitrocellulose matrix by nitroglycerine. Thus, the proposed diffusion coefficient for the deterrent is assumed to be directly dependent on the nitroglycerine swelling  $\theta_{NG}$  being, in turn, dependent on the nitroglycerine concentration  $c_{NG}$ , in the nitrocellulose matrix. The presence of nitroglycerine leads to higher overall diffusion coefficients and diffusion rates of the deterrent than those occurring in the absence of nitroglycerine. In this last case the diffusion rate of deterrent can be well described with the assumed model, which in fact reflects the diffusion coefficient  $D_{D, \text{single base}}$  in the single base propellants. For double base propellants, in the zones where nitroglycerine concentration is high, nitroglycerine swelling is maximal ( $\theta_{NG} \cong 1$ ) and the diffusion rate is reflected mainly by the diffusion coefficient  $D_{D, \text{double base}}$  in the swollen nitrocellulose matrix. The following chapter will describe the diffusion processes in double base propellants where  $D_{D,total} \cong D_{D, \text{double base}}$  because  $D_{D, \text{double base}} \gg D_{D, \text{single base}}$  [3,4] and consider the further acceleration of the diffusion rate of nitroglycerine in the presence of the deterrent.

#### 4.2.3.2 Investigation of the possible acceleration of nitroglycerine diffusion rate in the presence of deterrent

Type and concentration of deterrent and blasting oil were found to influence the value of the diffusion coefficient significantly [3,4], the diffusion processes of both migrants are therefore differently influenced by the temperature and their concentrations. The deterrent and nitroglycerine concentration profiles present in the propellant before the ageing are shown in Fig. 1B. During accelerated ageing, the nitroglycerine will diffuse from the region of highest concentration (zone II) into both directions. However, the nitroglycerine diffusion rate into zone I is much higher than the diffusion rate towards the NC-core (zone III). The change of the concentration of the deterrent and nitroglycerine diffusing inside the nitrocellulose matrix can be described by the general equation (8). In the case of the deterrent 'D', one can assume that the diffusion coefficient is influenced by the temperature 'T', deterrent concentration  $c_D$  and nitroglycerine concentration  $c_{NG}$ . Therefore, the equation describing the diffusion of the deterrent 'D' can be simplified to:

$$\frac{\partial c_D}{\partial t} = \frac{\partial}{\partial r} \left( D_D(c_D, c_{NG}, T) \frac{\partial c_D}{\partial r} \right) + \frac{g}{r} D_D(c_D, c_{NG}, T) \frac{\partial c_D}{\partial r} \quad (12)$$

In the case of the nitroglycerine, similarly, equation (8) for the diffusion of 'NG' reads:

$$\frac{\partial c_{NG}}{\partial t} = \frac{\partial}{\partial r} \left( D_{NG}(c_D, c_{NG}, T) \frac{\partial c_{NG}}{\partial r} \right) + \frac{g}{r} D_{NG}(c_D, c_{NG}, T) \frac{\partial c_{NG}}{\partial r} \quad (13)$$

The temperature dependence of the diffusion coefficient is assumed to fulfil the Arrhenius equation describing thermally activated processes. To take into account the interaction of both migrants in the nitrocellulose matrix, the following expression can be formulated [16]:

$$D(c, T) = D_0(c) \exp \left[ - \frac{\Delta E(c)}{RT} \right] \quad (14)$$

where

$$D_0(c) = D_0' \exp(U \cdot c + V \cdot c^2) \quad (15)$$

and

$$\Delta E = \sum_{i=0}^2 Q_i \cdot c^i \quad (16)$$

mean the preexponential factor and the activation energy of the diffusion, respectively. R stays for the gas constant ( $R=8.314 \text{ J}/(\text{mol}\cdot\text{K})$ ) and U, V and  $Q_i$  are parameters characterizing the dependence of the diffusion coefficients on the concentration of the migrants. For the diffusion of deterrent and nitroglycerine in EI-propellants, the following simplified assumption that  $V = Q_1 = Q_2 = 0$  and  $E = Q_0$  results in following approximations approximation

- For the migration of deterrent

$$D_D(c_D, c_{NG}, T) = D_{0,D} \cdot \exp(U_1' \cdot c_D + U_2' \cdot c_{NG}) \exp \left[ - \frac{E_D}{RT} \right] \quad (17)$$

- For the migration of nitroglycerine

$$D_{NG}(c_D, c_{NG}, T) = D_{0,NG} \cdot \exp(U_1'' \cdot c_D + U_2'' \cdot c_{NG}) \exp\left[-\frac{E_{NG}}{RT}\right] \quad (18)$$

At constant temperature above equations read:

- for the deterrent:

$$D_D(c_D, c_{NG}, T) = D_D \cdot \exp(U_1' \cdot c_D + U_2' \cdot c_{NG}) \quad (19)$$

- for the nitroglycerine:

$$D_{NG}(c_D, c_{NG}, T) = D_{NG} \cdot \exp(U_1'' \cdot c_D + U_2'' \cdot c_{NG}) \quad (20)$$

As mentioned above the presence of both, polymeric deterrents and nitroglycerine in nitrocellulose-matrix leads to the higher diffusion rates than if the migrants would be alone as in the single base propellants [3-4]. However, in case of nitrocellulose-blasting oil matrix (EI-propellants), once the matrix is swollen (mainly due to NG), it is important to determine the process of interactions/synergy between deterrent and nitroglycerine and its influence on the diffusion coefficients and particular diffusion rates. At the beginning of simulations we have assumed that the diffusion coefficients of the deterrent  $D_D$  and nitroglycerine  $D_{NG}$  are both dependent on the  $c_D$  and  $c_{NG}$  concentrations (Eqs. 19-20). However, the results of the optimization performed to minimize the sum of the squared difference between the measured and the calculated values brought the two parameters  $U_2'$  and  $U_2''$  towards zero and adjusted only the other parameters  $D_D$ ,  $U_1'$ ,  $D_{NG}$  and  $U_1''$ . This means that in order to obtain the best fit the model requires essentially only the deterrent concentration evolution.

To check this assumption two additional verifications were carried out:

(i) The first one by forcing the diffusion coefficients of both, deterrent and nitroglycerine to be dependent on the concentration profile of NG along the penetration depth. This can be done by fitting only the parameters:  $D_D$ ,  $U_2'$ ,  $D_{NG}$  and  $U_2''$  (with  $U_1' = U_1'' = 0$ ) (Eqs. 19-20). Simulations of the deterrent and nitroglycerine concentration profile dependence on propellant aging time are presented in figure 2. The symbols represent the experimentally determined concentrations of both migrating components at 71°C just after impregnation by the deterrent (labelled as 0) and after 4 weeks of aging (labelled as 4), the lines depict the simulated dependences after 0, 1, 2, 3 and 4 weeks. It can be observed that in the case of the assumption (i) it is impossible to describe the measured evolution of the concentration profiles of both deterrent and nitroglycerine - note the difference between experimental points (empty circles) after 4 weeks and simulation results for this aging time drawn as bold lines.

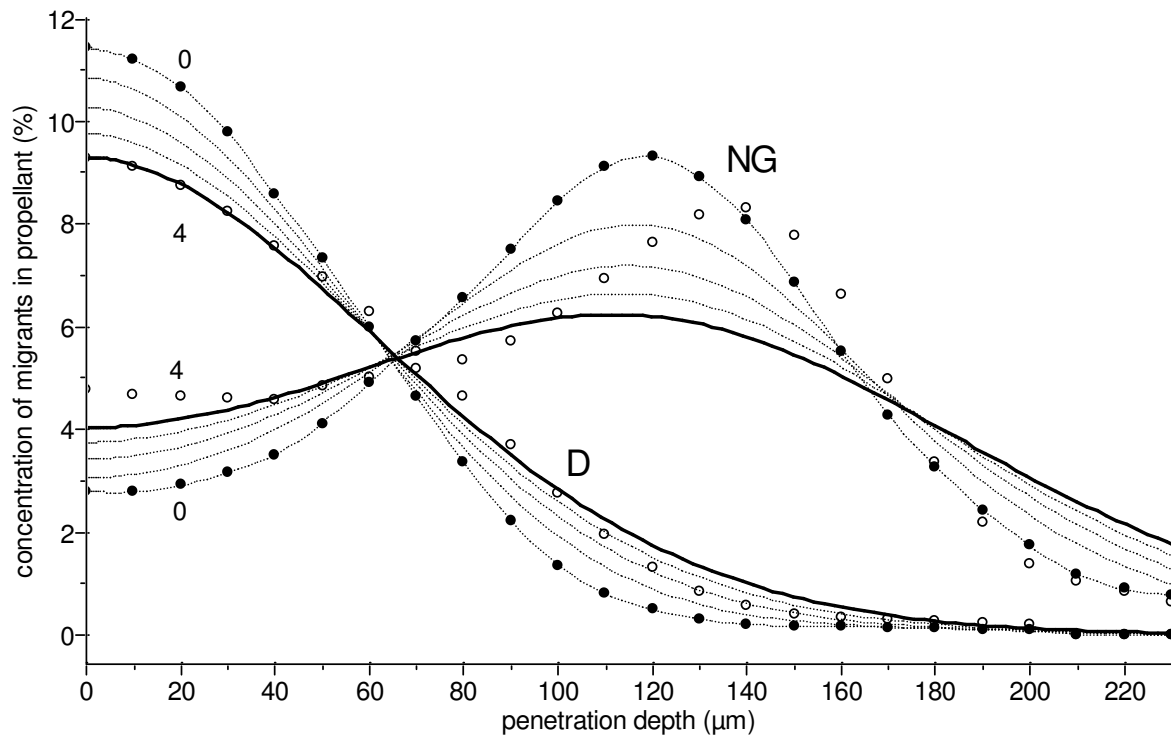


**Fig. 2** Concentration profiles of detergent and nitroglycerine in unaged EI-propellant (0) and in aged EI-propellant stored at 71°C for 4 weeks (4). The diffusion tends to level out the concentration gradient within the zone up to ca 130  $\mu\text{m}$ . Almost no diffusion of nitroglycerine takes place from the end of that zone towards the NC-core. However, the simulation shows that it is impossible to describe correctly the migration process if the diffusion coefficients are expressed as a function of the nitroglycerine concentration profile. The experimental points obtained after 4 weeks are presented as empty circles, the simulation lines for this aging time are drawn in bold.

(ii) The second one by letting the diffusion coefficients of both detergent and nitroglycerine to be dependent on the concentration profile of detergent along the penetration depth. It was done by fitting the parameters:  $D_D$ ,  $U_1'$ ,  $D_{NG}$  and  $U_1''$  (with  $U_2' = U_2'' = 0$ ) (Eqs. 19-20). Simulations of the detergent and nitroglycerine concentration profile dependence on propellant aging time are presented in figure 3. Annotations are the same as in figure 2. However, it can now be observed that the model can accurately describe the measured evolution of the concentration profiles of both detergent and nitroglycerine taking into account the influence of the concentration profile of the detergent only on the diffusion coefficients. This observation is in accordance with previous optimization tending to bring parameters  $U_2'$  and  $U_2''$  towards zero during the optimization process to obtain the best fit. Note that in order to have a model with as less parameters as possible we just have set  $U_2' = U_2'' = 0$  in the current optimization.

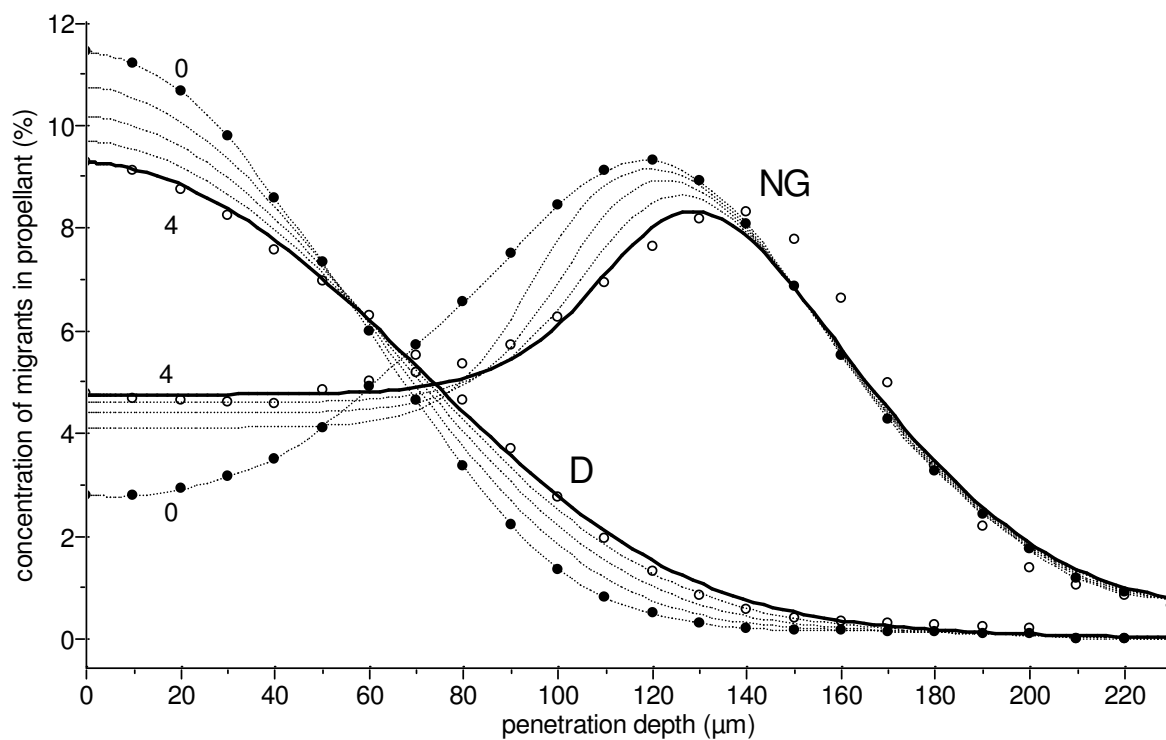


**Fig. 3** Concentration profiles of detergent and nitroglycerine in unaged EI-propellant (0) and in aged EI-propellant stored at 71°C for 4 weeks (4). The diffusion tends to level out the concentration gradient within the zone up to ca 130  $\mu\text{m}$ . Almost no diffusion of nitroglycerine takes place from the end of that zone towards the NC-core. Contrary to the results depicted in Fig.2 present simulation accurately describes the migration process of both detergent and nitroglycerine after assumption that the diffusion coefficients depend on the detergent concentration profile. The experimental points obtained after 4 weeks are presented as empty circles, the simulation lines for this aging time are drawn in bold.

Results of these simulations are in very good accordance with the experimental observation that presence of detergent results in faster diffusion rates of nitroglycerine in nitrocellulose matrix. The increase of the diffusion coefficient of the zone with high detergent concentration (up to penetration depth of ca. 60  $\mu\text{m}$ ) leads to increase of the nitroglycerine concentration in this zone (see change of the concentration of both migrants versus time in outer zone of the grain shown in Fig.3). This result confirms that the proper choice of the appropriate polymeric detergent is crucial for preparing propellant with superior performance concerning the ballistic stability.

Calculation results are consistent with the observation (see Fig.3) that, at the penetration depth of 160  $\mu\text{m}$  when the NG concentration amounts to about 5% NG, in the absence of detergent the migration rate of NG is very low. Concentration of NG remains at ca. 5% after 4 weeks at 71°C. However, at the penetration depth of 20  $\mu\text{m}$  with about 3% NG and ca. 11% initial detergent concentration, the migration rate of NG is very high. Concentration of NG increases from 3% to about 5% after 4 weeks at 71°C. This observation confirms the strong influence of the detergent concentration on the rate of nitroglycerine migration and additionally indicates that the diffusion in the nitrocellulose matrix in the presence of both plasticizers is faster than in the case one migrant only.

To estimate the diffusion coefficients, non linear regression algorithms were applied for best fitting of the experimental data points presented in Fig.3. During this procedure, the parameters were progressively varied in order to minimise the sum of the squared difference between the measured and the calculated values. The calculated dependence of both diffusion coefficients on the deterrent concentration at 71°C is depicted in Fig.4. The diffusion coefficients for the deterrent and blasting oil at 71°C amounted respectively to  $D_D=2.55 \cdot 10^{-16} \text{ m}^2/\text{s}$ ,  $U'_1=3.65 \cdot 10^{-2} \%^{-1}$ ,  $D_{NG}=2.69 \cdot 10^{-17} \text{ m}^2/\text{s}$ ,  $U''_1=7.69 \cdot 10^{-1} \%^{-1}$  (Eqs. 19-20). The approach presented in this chapter and used for simulations fits the experimental data best, however, should be verified by other experimental data.

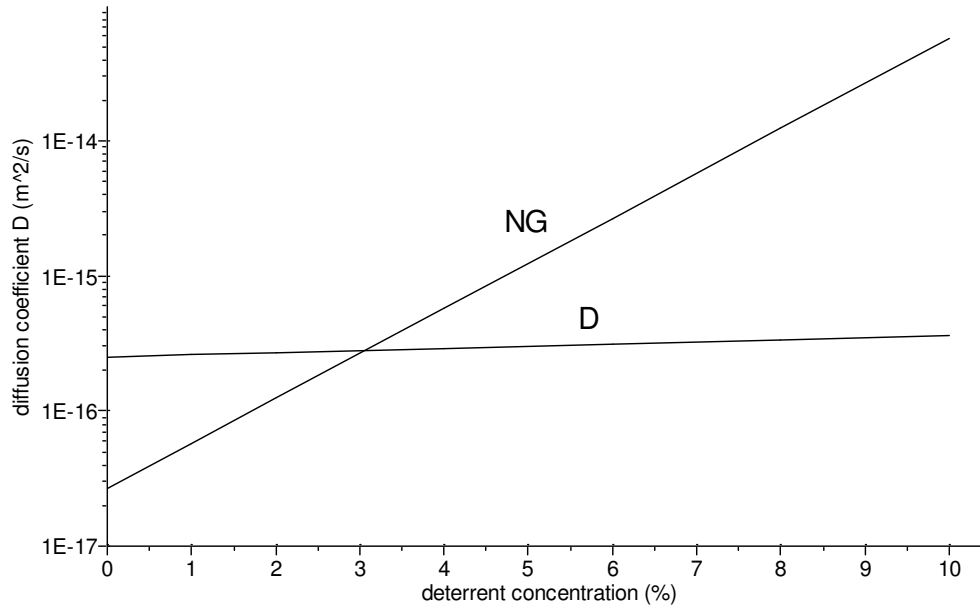


**Fig. 4** Diffusion coefficient at 71°C of deterrent (D) and nitroglycerine (NG) as a function of the deterrent concentration. A high concentration of deterrent considerably increases the value of the diffusion coefficient of nitroglycerine and significantly less those of the deterrent. As a result the deterrent tends to level out the nitroglycerine concentration gradient within the region where its concentration is significant. However no diffusion of nitroglycerine takes place in the zone where the deterrent is absent (see Fig 3).

Taking into account the presented results of the simulation and their very good fit of experimental data the migration process during thermal aging of the double base propellant can now be interpreted as following. The deterrent diffuses from the surface of the grains towards the centre which results in a progressive decrease of its concentration in the outer layer of the grains. The increase of the deterrent concentration in the inner part of grains induces a progressive increase of the diffusion coefficient of the nitroglycerine. During prolonged aging the concentrations of both, deterrent and nitroglycerine tend to equalize along the grain radius. However, as soon as the diffusion front of the nitroglycerine moves towards the inner zone of the propellant grain where only single base propellant is present, its diffusion rate decreases. In the absence of nitroglycerine in the propellant core and, therefore the absence of propellant swelling, the diffusion of both nitroglycerine and deterrent is very slow as in the single base propellant where  $D_{NG}=2.69 \cdot 10^{-17} \text{ m}^2/\text{s}$ .

The results presented in Figs. 2 and 3 demonstrate the potential of application of the numerical analysis for the simulation of migration in the systems where migrants may interact during diffusion. The simulations can be successful despite the fact that the diffusion coefficients of both migrants are strongly dependent on each other concentration.

#### 4.2.3.3 Temperature variations

Propellant often undergoes temperature fluctuations during their shelf life or final use. The diffusion coefficient  $D$  of the migrants varies exponentially with the temperature. It is therefore important that predictive tools enable the simulation of the diffusion under real conditions, as a small temperature increase can induce a faster migration. Below we report the results of the simulation of the deterrent diffusion in the propellant matrix at different temperature modes.

Simulations were carried out for the double base ball powder propellant K 5810, lot O2MQ (5.56 mm cartridges produced in Germany containing a lead free primer (“Sintox”)) [5]. The flattened grains of propellant can be geometrically represented by an ellipsoid with a great axis of 660 $\mu\text{m}$  and with two small axis of 360  $\mu\text{m}$ . Propellant contains around 10% of nitroglycerine and is stabilized with DPA. Dibutylphthalate (DBP) was applied as deterrent. The simulations were compared with the experimental data presented in [5] reporting the values of the diffusion coefficients which amount to  $4.1 \cdot 10^{-18}$ ,  $3.3 \cdot 10^{-17}$ ,  $9 \cdot 10^{-17}$ ,  $2 \cdot 10^{-16}$  and  $7.2 \cdot 10^{-16}$   $\text{m}^2/\text{s}$  at 50, 60, 65, 70 and 80 $^{\circ}\text{C}$ , respectively. Based on these values, following diffusion coefficients  $D_{D,0} = 2.06 \cdot 10^9$   $\text{m}^2/\text{s}$  and  $E_D = 164.7$   $\text{kJ/mol}$  can be calculated. Determined parameters can then be applied for estimating the value of the diffusion coefficient at any new temperatures and the corresponding concentration profile at any time. The change of the deterrent concentration profiles occurring during accelerated aging at 80 $^{\circ}\text{C}$  are presented in figure 5 depicting additionally the experimental data (displayed as symbols) collected for non aged sample.

The simulated curves presented in Fig.5 cross in the semi-isoconcentration point laying approximately 25-30  $\mu\text{m}$  from the surface. One can distinguish two zones separated by the vertical line arbitrarily drawn at the penetration depth of 25  $\mu\text{m}$ . In the left zone (I), laying between the surface and 25  $\mu\text{m}$ , the concentration of the deterrent decreases during the aging due to the diffusion of the deterrent into the core of the grain. Contrary, in the second zone (II) the amount of deterrent during aging continuously increases in the region between ca. 25-30 and approximately 150  $\mu\text{m}$ . The average concentration of the deterrent in both zones before aging is displayed by dashed horizontal lines. The average concentrations of deterrent in fresh sample and after 10 days of aging are additionally presented in the inset for both propellant zones (I) and (II), respectively.

The concentration profiles of the deterrent along the grain radius depend on the initial deterrent concentration profile and on the temperature. The simulation of the aging time under different temperature modes carried out in order to predict the same concentration on the surface as in the isothermal experiments will therefore result in the simulation of the same concentration profile inside the propellant grain. The results of such simulations are presented in Table 1 showing the aging time

required to reach the same deterrent concentrations under different temperature profiles as those obtained in isothermal conditions at 80°C after different times during 10 day aging.

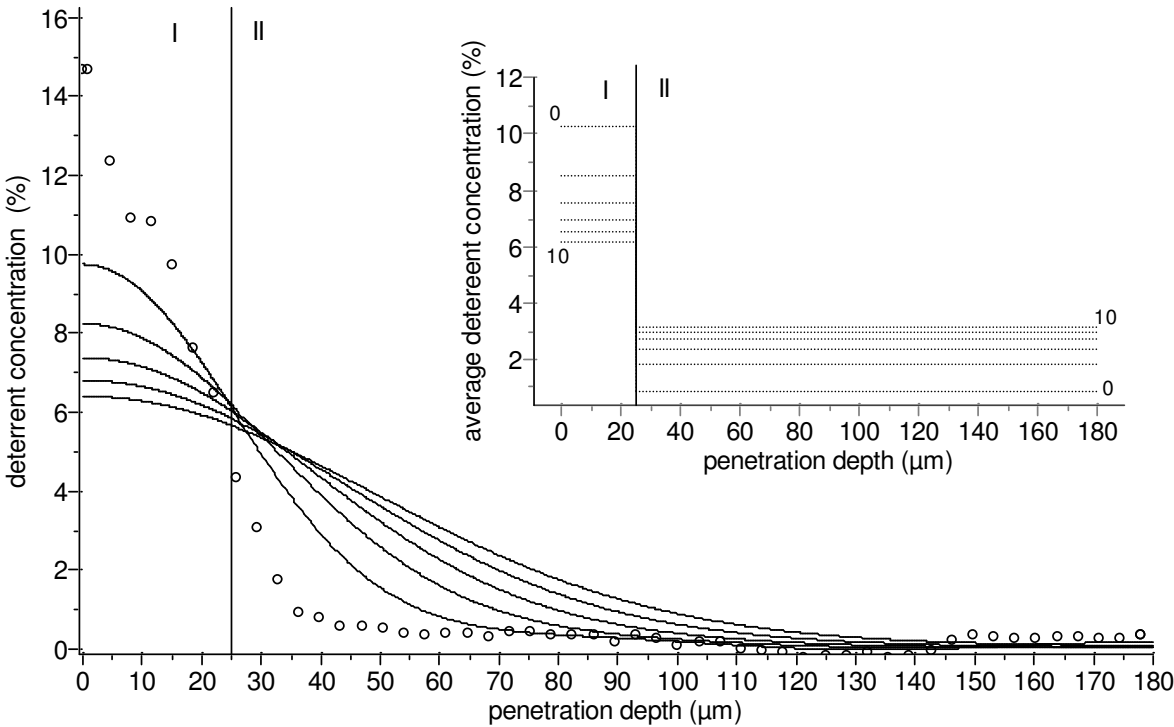


**Fig. 5** Initial experimental (symbols, data source: Royal Military Academy, Bruxelles, Belgium) and simulated (lines) concentration distribution of deterrent (DBP) in a double base ball powder propellant during an accelerated aging at 80°C. Aging times in the range of 0-10 days are marked on curves. The average concentrations of deterrent in zones (I) and (II) after aging time between 0 and 10 days are displayed in the inset.

**Tab. 1** Comparison of the times at which during aging carried out under different temperature profiles the same deterrent concentration profiles are reached as those obtained at 80°C after 2, 4, 6, 8 and 10 days.

Surface concentration (%)	9.7	8.2	7.4	6.8	6.4
80°C (days)	2	4	6	8	10
70°C (days)	10.31	20.56	30.82	41.08	51.29
60°C (months)	1.92	3.82	5.73	7.64	9.54
50°C (years)	1.01	2.01	3.01	4.01	5.01
40±20°C, 24h period (years)	0.74	1.47	2.20	2.93	3.66
40°C (years)	7.12	14.21	21.3	28.39	35.45
30°C (years)	57.42	114.56	171.70	228.83	285.69
Stanag 2895 / A1 (years)	0.65	1.59	2.56	3.54	4.53

The results presented in Tab.1 indicate that the deterrent concentration profile in the investigated propellant after e.g. 10 days of aging at 80°C will be equivalent to those obtained after ca.

35.5 years of aging at 40°C or 3.7 years of aging at 40°C with  $\pm 20^\circ\text{C}$  24h period. Due to the fact that the ballistic performance may depend on the deterrent concentration profile its knowledge may help in evaluation after which shelf life time the ballistic requirements will be still fulfilled.

Using the AKTS-SML software it is also possible to simulate the concentration of the deterrent in certain grain zone after arbitrarily chosen aging time and under any temperature profiles such as stepwise variations, oscillatory conditions, temperature shock, or even real atmospheric temperature profiles. This is especially important for accurate migration simulation under real conditions of use as the propellants undergo different temperature variation during its manufacture, storage or final usage. Such simulation is presented in Fig.6 where the average deterrent concentration in the inner zone (zone II, see Fig.5) is simulated for three temperature profiles:

(i) at constant temperature of 40°C

(ii) at 40°C with  $\pm 20^\circ\text{C}$  amplitude. The temperature oscillates between 20 and 60°C with a sinusoidal period of 24 h to reproduce the day/night variation

(iii) for the high temperature climatic category A1 according to the STANAG 2895 [2]. This document describes the principal climatic factors which constitute the distinctive climatic environments found throughout the world and provides guidance on the drafting of the climatic environmental clauses of requirement documents.

The curves depicted in Fig.6 indicate that although the average temperature is 40°C in simulations (i) and (ii), the average deterrent concentrations in zone II are clearly different in both cases. After two years of the storage the deterrent concentration amounted to ca. 1.2; 2.4 and 2.6% for the temperature profiles (i), (iii) and (ii), respectively. The periodic variations of the temperature in case (iii) significantly increased the amount of migrated deterrent in the zone II compared to the migration under isothermal conditions occurring at the temperature profile (i). The concentration of deterrent in the zone II is more than two times larger if the average temperature of 40°C has oscillated with the amplitude of 20°C. Presented simulations indicate that migration of the deterrent in the propellant strongly depends on the exact temperature profile during shelf life. Even if the arithmetic mean temperature of the oscillatory temperature mode is the same as in isothermal conditions, the temperature amplitudes greatly influence the deterrent diffusion rate. This indicates clearly that the underestimation of the temperature effects during storage can lead to the severe changes of the deterrent concentration towards the centre of the pellet, what, in turn, will influence the ballistic properties of the propellants.

In the third simulation applying the temperature profile (iii), by implementing climatic variations into the programme, it was possible to forecast the average deterrent concentration for different climates. The curve labelled Stanag A1 in Fig.6 depicts the time dependence of the average deterrent concentration in zone II (see Fig.5) in the high climatic category A1 for the meteorological storage/transit temperature profiles according to STANAG 2895 (see Fig. 6, inset) [2]. This meteorological temperature illustrates the ambient air temperature measured under standard

conditions, whereas storage and transit temperature represents the air temperature measured inside temporary unventilated field shelter e.g. in railway boxcar which is exposed to direct solar radiation.

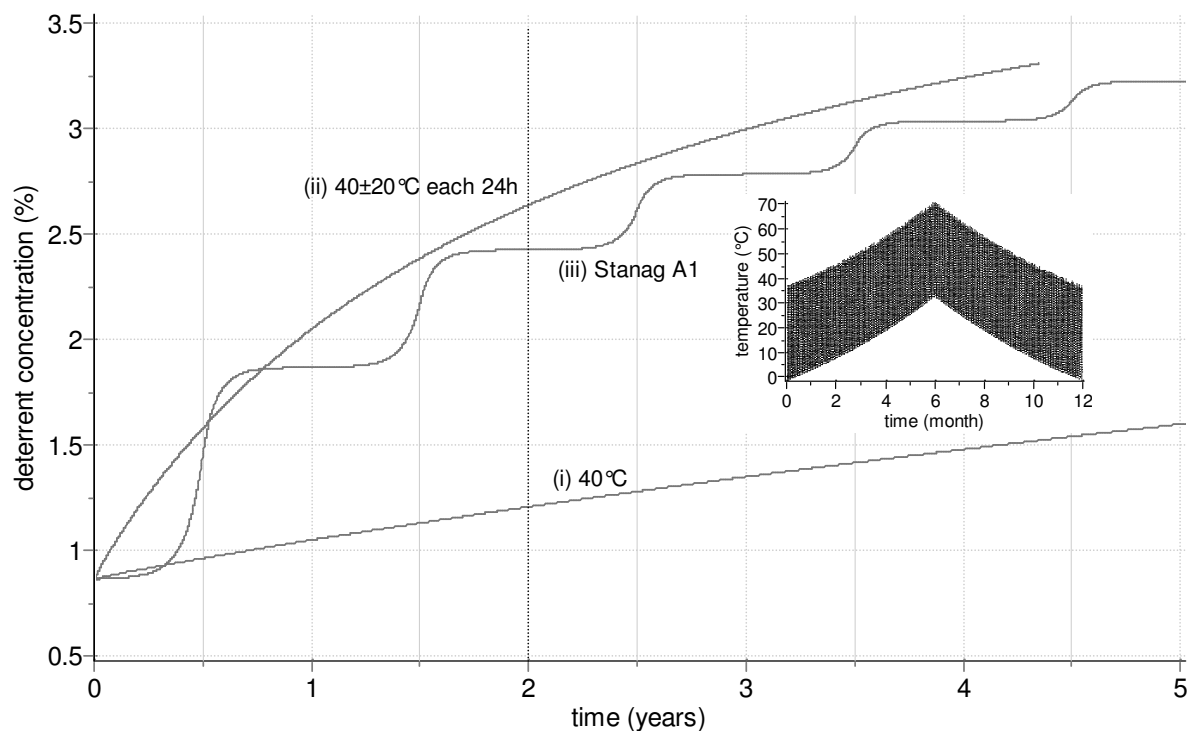


**Fig. 6** Average concentration of detergent in zone II (see Fig.5) in double base propellant as a function of aging time under isothermal ( $40^{\circ}\text{C}$ ), oscillatory ( $40^{\circ}\text{C}\pm 20^{\circ}\text{C}$ , 24 h period) temperature conditions and high climatic category A1 according to STANAG 2895. The storage/transit temperatures recorded during one year in the climatic category A1 are presented in the inset.

## Conclusion

This study has demonstrated some advantages and possibilities of the numerical approximation of the diffusion process of blasting oil and detergent through the propellant matrix. The results of simulations and their good fit to experimental data indicate that it was possible to simulate the diffusion processes even in the case when additional phenomenon was present namely the variation of the diffusion coefficients in dependence of the plasticizers concentration, being in the simpler cases dependent on the temperature only. By introducing to the expression of the nitroglycerine and detergent diffusion coefficients the additional concentration terms it was possible to successfully simulate how the  $D$  value progressively decreases with the penetration depths of the detergent front within the NC corn.

Results of these simulations are in very good accordance with the experimental observation that presence of detergent results in faster diffusion rates of nitroglycerine in nitrocellulose matrix. On the other hand, the influence of the NG concentration on the diffusion process is significantly smaller as illustrated by the results of simulation depicted in Figs.2 and 4. The simulations indicate that the blasting oil diffuses faster in zones with detergent than in the regions with zero detergent concentration. Comparison of the experimental results with the simulated migration curves shows their excellent fit. This confirms that application of diffusion modelling is correct even under such experimental

conditions where the diffusion coefficient of the migrant is not constant during the aging time. Presented results demonstrated clearly that a small temperature variation, even over a short period of time, can lead to large deviations in the concentration profiles of diffusing deterrent. Additionally, the diffusion modelling software allowed simulating the time dependence of the average deterrent concentration in the inner zone of the propellant grains during storage at arbitrarily chosen temperature profiles including STANAG 2895.

## References

- [1] Advanced Kinetics and Technology Solutions, AKTS AG : <http://www.akts.com> (AKTS-SML software).
- [2] STANAG 2895 (1990), Extreme climatic conditions and derived conditions for use in defining design/test criteria for NATO forces material, <http://www.nato.int/docu/stanag/2895/2895.pdf>.
- [3] B. Vogelsanger, B. Ossola and E. Brönnimann, Propellants, Explos., Pyrotech., 21 (1996) 330.
- [4] B. Ossola, B. Vogelsanger and E. Brönnimann, 25th International Annual Conference of ICT, Karlsruhe, Germany (1994).
- [5] L. Jeunieu, M. H. Lefebvre, P. Guillaume, S. Wilker, S. Chevalier and S. Eibl, Proc. Int. Ann.Conf. ICT, 35 (2004) 15.
- [6] E. Varriano-Marston, J. Appl. Polym. Sci., 33, (1987) 107.
- [7] B. Roduit, L. Xia, P. Folly, B. Berger, J. Mathieu, A. Sarbach, H. Andres, M. Ramin, B.Vogelsanger, D. Spitzer, H. Moulard and D. Dilhan, J. Therm. Anal. Cal., 93 (2008) 143.
- [8] D. S. Ellison and A. Chin, Proc. 6<sup>th</sup> Int. Symp. HFC on Energetic Materials, Fraunhofer ICT, Pfinztal-Berghausen, Germany, May (2008) 303.
- [9] U.Ticmanis, P. Guillaume, S. Wilker, G. Pantel, A. Fantin, M. Koch and L. Jeunieu, Proc. 6<sup>th</sup> Int. Symp. HFC on Energetic Materials, Fraunhofer ICT, Pfinztal-Berghausen, Germany, May (2008) 315.
- [10] B. Roduit, P. Guillaume, S. Wilker, P. Folly, A. Sarbach, B.Berger, J. Mathieu, M.Ramin and B.Vogelsanger, Proc.6<sup>th</sup> Int. Symp. HFC on Energetic Materials, Fraunhofer ICT, Pfinztal-Berghausen, Germany, May (2008) 67.
- [11] J. Crank, The Mathematics of Diffusion, 2nd edition, Oxford University Press, New York, 1975.
- [12] J.M. Vergnaud, Liquid Transport Processes in Polymeric Materials, Prentice Hall, London, 1991.
- [13] M. Abramowitz and A. Stegun, Handbook of mathematical functions, Dover Publications, New York, 1972, p. 371, eq 9.5.12
- [14] P.R. Bevington, Data Reduction and Error Analysis for the Physical Sciences, 2nd edition, Mc Graw-Hill, Boston, 1992, p 162-163.
- [15] M.E. Levy, Report R-1286 (1955), Pitman-Dunn Laboratories, Frankford Arsenal, Philadelphia, USA.
- [16] A. Ochsner, J. Gegner and G. Mishuris, Metal Science and Heat Treatment 46 (2004) 148.